Available online www.jsaer.com

Journal of Scientific and Engineering Research, 2024, 11(7):8-16

Research Article

ISSN: 2394-2630
CODEN(USA): JSERBR

Theoretical study of the characteristics of the current – voltage of a homojunction of $CuInSe_2$ deposited on a CdTe substrate in the presence of an additional electric field of 2.105 Vcm^{-1}.

Yves Tabar, Abdoul Aziz Correa, Elhadji Mamadou Keita, Fallou Mbaye, Babacar Mbow

Laboratory of Semiconductors and Solar Energy, Physics Department, Faculty of Science and Technology
University Cheikh Anta DIOP-Dakar-SENEGAL

Abstract The objective of this work is to do the theoretical study of the current – voltage characteristics of a homojunction deposited on a substrate [$CuInSe_2$(N)/$CuInSe_2$(P)/CdTe (P+)] in the presence of an additional electric field of 2.105 Vcm^{-1}. The additional internal electric field is due to a doping gradient. In this case we establish the calculation of the different expressions of the respective photocurrent by solving the continuity equations which govern the variation of the minority carriers in each region and by using the boundary conditions. A simulation of this photocurrent depending on the voltage is made by keeping the same values of the geometric parameters. The results obtained shows that the maximum photocurrent is approximately equal to 27.5 $mA.cm^{-2}$ at low values of the voltage and that the maximum power is approximately equal to 7.329 mW. Then, we studied the influence of the series resistance, the shunt resistance and the ideality factor. We observe that the increase in the series resistance decreases the slope of the current-voltage characteristic, the increase in the shunt resistance is manifested by an increase in the open-circuit voltage and as well as the ideality factor. Our results are according with those found in the literature.

Keywords Thin films, $CuInSe_2$, CdTe, Electrical Characteristics, Photodiode, Electric field

Introduction

Photovoltaic conversion is the transformation of light energy into electrical energy. Devices capable of performing this transformation are called solar cells. Their internal quantum efficiency were relatively very low, which gave motivation to study the limiting factors of the photovoltaic conversion [1].

Theoretical Study

Modelling

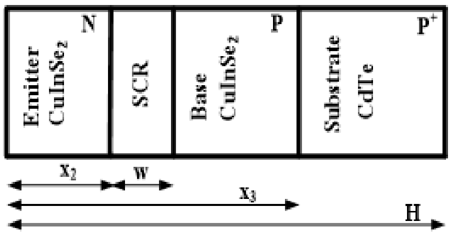

Figure 1: Diagram of the structure: $CuInSe_2$(N)/$CuInSe_2$(P)/CdTe (P^+)

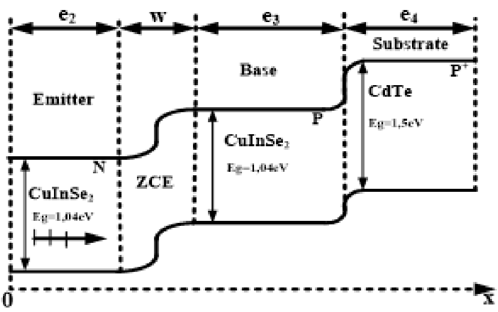

Figure 2: Energy band diagram of the structure: $CuInSe_2$ (N)/$CuInSe_2$(P)/CdTe (P^+)

In order to simulate a homojunction model corresponding to an N-P junction deposited on a doped substrate P+, we assume that the junction is between the two first layers and that the thickness of the substrate is infinitely large compared to the others geometrical parameters.

Figures 1 and 2 respectively represent the structure and the band diagrams of a homojunction model N-P deposited on a P+ type substrate. In Figure 2: e2, e3 and e4 respectively represent the thicknesses of the emitter, the base and the substrate and w represents the thickness of the space charge region. In figure 1 we have x2 = e2, x3=e2 + w + e3 and H = e2+ w + e3 + e4.

Expression of the photocurrent in the emitter

The variation of the holes in the n-type emitter in static regime is determined by the continuity equation (1) [2,3,4]:

$$\frac{d^2\Delta p_2}{dx^2} - \frac{\mu_{p2}.E}{D_{p2}}\frac{d\Delta p_2}{dx} - \frac{\Delta p_2}{L_{p2}^2} + \frac{\alpha_2 N(1-R)e^{\alpha_2 x}}{D_{p2}} = 0 \quad (1)$$

With μp_2 the holes mobility, E the electrical field, Lp_2 the diffusion length of the holes in the emitter, α_2 the absorption coefficient of $CuInSe_2$, Dp_2 the diffusion coefficient of the holes in the emitter, N incident photon number and R the reflection coefficient.

The general solution of equation (1) is of the type:

$$\Delta p_2(x) = Ae^{r_1 x} + Be^{r_2 x} + Ke^{-\alpha_2 x} \quad (2)$$

$$\text{With}\begin{cases} r_1 = \dfrac{\frac{\mu p_2.E}{Dp_2} + \sqrt{\left(\frac{\mu p_2 E}{Dp_2}\right)^2 + \left(\frac{2}{Lp_2}\right)^2}}{2} \\ r_2 = \dfrac{\frac{\mu p_2.E}{Dp_2} - \sqrt{\left(\frac{\mu p_2 E}{Dp_2}\right)^2 + \left(\frac{2}{Lp_2}\right)^2}}{2} \end{cases}$$

A, and B are constants and $K = -\frac{\alpha_2 N(1-R)}{D_{p2}(\alpha_2^2 + \frac{\mu E}{Dp_2}\alpha_2 - (\frac{1}{Lp_2})^2)}$

Thus, by determining constants *A* and *B*, the boundary conditions are on below:

$$Dp_2\frac{d\Delta p_2}{dx} - \mu_{P2}.E.\Delta p_2 = Sp_2.\Delta p_2 \qquad pour \quad x = 0 \quad (3)$$

$$\Delta p_2 = 0 \qquad pour \quad x = x_2 \quad (4)$$

We obtain the expression of the photocurrent in the emitter given by:

$$J_e = \frac{q\alpha_2 N(1-R)L}{(\alpha_2 + \frac{1}{l})^2 L^2 - 1}\left\{\frac{e^{\frac{x_2}{l}}\left(\alpha_2 L + \frac{Sp_2 L}{Dp_2} + \frac{2L}{l}\right) - e^{-\alpha_2 x_2}\left[\left(\frac{Sp_2 L}{Dp_2} + \frac{2L}{l}\right)\cosh(\frac{x_2}{L'}) + (\frac{Sp_2 L^2}{Dp_2 l} + \frac{L^2}{l^2} + 1)\sinh(\frac{x_2}{L'})\right]}{\cosh(\frac{x_2}{L'}) + (\frac{Sp_2 L}{Dp_2} + \frac{L}{l})\sinh(\frac{x_2}{L})} - \alpha_2 L e^{-\alpha_2 x_2}\right\} \quad (5)$$

With $l = \frac{2Dp_2}{\mu p_2.E}$ and $L' = \frac{l.Lp_2}{\sqrt{(Lp_2^2 + l^2)}}$

Expression of the photocurrent in the space charge region

This component of the photocurrent is due to the carriers created only in the space charge region. It is given by equation (5) [6,7]:

$$J_{zce} = qN(1-R)(1 - e^{-\alpha_2 w})e^{-\alpha_2 x_2} \quad (6)$$

Expression of the quantum photocurrent in the base

The continuity equations reflecting the variation of electrons generated in the base and in the substrate are given by equations (6) and (7) [5]:

$$\frac{d^2\Delta n_3}{dx^2} - \frac{\Delta n_3}{Ln_3^2} = -\frac{\alpha_3 N(1-R)e^{-(\alpha_2 - \alpha_3)(x'_2 + w_1)}}{Dn_3}e^{-\alpha_3 x} \quad (7)$$

$$\frac{d^2\Delta n_4}{dx^2}-\frac{\Delta n_4}{Ln_2{}^2}=-\frac{\alpha_4 N(1-R)e^{-(\alpha_2-\alpha_3)(x'_2+w_1)}e^{-(\alpha_3-\alpha_4)x_3}}{Dn_4}e^{-\alpha_4 x} \tag{8}$$

α_4 is the absorption coefficient of CdTe, Ln_4 is the diffusion length of electrons in the substrate, Dn_4 coefficient of electron diffusion in the substrate.

The general solutions of equations (6) and (7) are of the type [8]:

$$\Delta n_3(x)=A_1 e^{\frac{x}{Ln_3}}+B_1 e^{\frac{-x}{Ln_3}}+K_1 e^{-\alpha_3 x} \tag{9}$$

$$\Delta n_4(x)=A_2 e^{\frac{x}{Ln_4}}+B_2 e^{\frac{-x}{Ln_4}}+K_2 e^{-\alpha_4 x} \tag{10}$$

With A_1 , A_2 , B_1 and B_2 constants and $\begin{cases} K_1=-\dfrac{\alpha_3 N(1-R)Ln_3{}^2 e^{-(\alpha_2-\alpha_3)(x'_2+w_1)}}{Dn_3(\alpha_3{}^2 Ln_3{}^2-1)} \\ K_1=-\dfrac{\alpha_4 N(1-R)Ln_4{}^2 e^{-(\alpha_2-\alpha_3)(x'_2+w_1)}e^{-(\alpha_3-\alpha_4)x_3}}{Dn_4(\alpha_4{}^2 Ln_4{}^2-1)} \end{cases}$

The constants are determined from the boundary conditions given by equations (8), (9), (10) and (11) [6,10]:

$$\Delta n_3=0 \quad \text{for} \quad x=x'_2+w_1 \tag{11}$$

$$Dn_3\frac{d\Delta n_3}{dx}=Dn_4\frac{d\Delta n_4}{dx} \quad \text{for} \quad x=x_3 \tag{12}$$

$$\Delta n_3=\Delta n_4 \quad \text{for} \quad x=x_3 \tag{13}$$

$$\Delta n_4=0 \quad \text{for} \quad x=H \tag{14}$$

The photocurrent describing the base contribution is given by equation (12):

$$J_b=\frac{\alpha_3 Ln_3 e^{-(\alpha_2-\alpha_3)(x'_2+w_1)}}{(\alpha_3{}^2 Ln_3{}^2-1)}\left\{\begin{array}{l}\alpha_3 Ln_3 e^{-\alpha_3(x_2+w)} \\ -\dfrac{(\alpha_3 Ln_3-\frac{Dn_3 Ln_4}{Dn_4 Ln_3})+\frac{\alpha_4 Ln_4(\alpha_3{}^2 Ln_3{}^2-1)(1-\alpha_4 Ln_4)}{\alpha_3 Ln_3(\alpha_4{}^2 Ln_4{}^2-1)}}{cosh(\frac{H-(x_2+w)}{Ln_3})+\frac{Dn_4 Ln_3}{Dn_3 Ln_4}sinh(\frac{H-(x_2+w)}{Ln_3})}e^{-\alpha_3 H} \\ -\dfrac{\left[sinh(\frac{H-(x_2+w)}{Ln_3})+\frac{Dn_4 Ln_3}{Dn_3 Ln_4}cosh(\frac{H-(x_2+w)}{Ln_3})\right]}{cosh(\frac{H-(x_2+w)}{Ln_3})+\frac{Dn_4 Ln_3}{Dn_3 Ln_4}sinh(\frac{H-(x_2+w)}{Ln_3})}e^{-\alpha_3(x_2+w)}\end{array}\right\} \tag{15}$$

The total photocurrent resulting from the contribution of the different regions is given by equation (16):

$$\boldsymbol{J_{total}=J_e+J_{zce}+J_b} \tag{16}$$

Determination of the Characteristic Parameters of a solar cell

Equivalent model of the solar cell

The equivalent electrical model of the solar cell is shown in Figure 4. In this figure, we note a current source and a diode in parallel with a series resistor which models the ohmic losses. We also note the presence of the shunt resistor which models the parasitic currents which cross the cell.

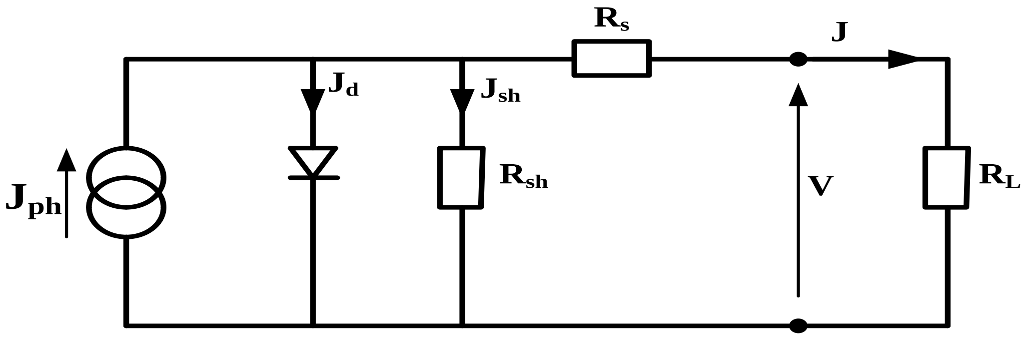

Figure 3: Equivalent electrical model of a solar cell in the presence of parasitic resistances

The current - voltage characteristic is represented by equation (17) [11; 12]:

$$J = J_{ph} - J_s\left[e^{\frac{e(V+R_S J)}{\eta kT}} - 1\right] - \frac{V+R_S\,J}{R_{sh}} \qquad (17)$$

With Jph is the photocurrent, Js is the diode saturation current, V is the voltage delivered by the solar cell, Rs is the series resistance, Rsh is the shunt resistance, K is the constant of Boltzmann, T is the temperature, n is the ideality factor.

The photocurrent Jph models the photogenerated current during absorption of incident photons. The shunt resistance Rsh models the leakage currents that exist in the structure. These leakage currents can take place along the periphery of the photodiode surface and through the emitter. The resistive losses in the semiconductor material and the contact resistances at the metal/semiconductor interfaces are modeled by the resistance Rs in series [14].

Determination of the short-circuit current (Jsc)

In the case of a real solar cell modelled by equation (18), the short-circuit current is no longer equal to the photocurrent generated, it is given by the following implicit relationship [13]:

$$J_{sc} = \frac{\eta KT}{qR_s} \times \ln\left(\frac{J_{ph}}{J_s} - \frac{J_{sc}}{J_s} - \frac{R_s J_{sc}}{R_{sh} J_s} + 1\right) \qquad (18)$$

The short-circuit current therefore depends on the shunt and series resistance.

Determination of open-circuit voltage (Vco)

It is the voltage from which the diode in the dark supplies a current equal to the short-circuit current J_{sc}. It is obtained from equation (19) [13]:

$$V_{co} = \frac{\eta KT}{q} \times \ln\left(\frac{J_{ph}}{J_s} - \frac{V_{co}}{R_{sh} J_s} + 1\right) \qquad (19)$$

It is independent of the series resistance.

Maximum Power Point Determination

The solar cell power is defined by the relation:

$$P = J \times V \qquad (20)$$

Where *J* is the current supplied by the solar cell and *V* the polarization voltage at its terminals.

Approximate resolution techniques are used to solve the various implicit equations. Considering that the space charge zone is located only between the n and p regions of each structure and that the electric field is zero outside this zone, the results obtained can be applied to the different structures considered.

The form factor FF

It defines the efficiency of the solar cell. It is obtained by the relation (21):

$$FF = \frac{P_m}{J_{sc} \cdot V_{co}} \qquad (21)$$

Where *Pm* is the power of operating point of the solar cell

The energy conversion efficiency

It is determined by the ratio between the maximum power generated and that of the incident solar radiation.

$$\eta_c = \frac{P_m}{P_{solaire}} \quad (22)$$

Where P_{solar} is the power of solar radiation (P_{solar} = 93,1 mW.cm^{-2} (AM 1) [12,13,14]

Results and Discussions

Absorption coefficients of the different materials used

For this structure, the theoretical model is proposed to determine the internal quantum efficiency. The variation of absorption coefficients of the materials ($CuInSe_2$ and CdTe) is given according to the energy by the figure 1 [9].

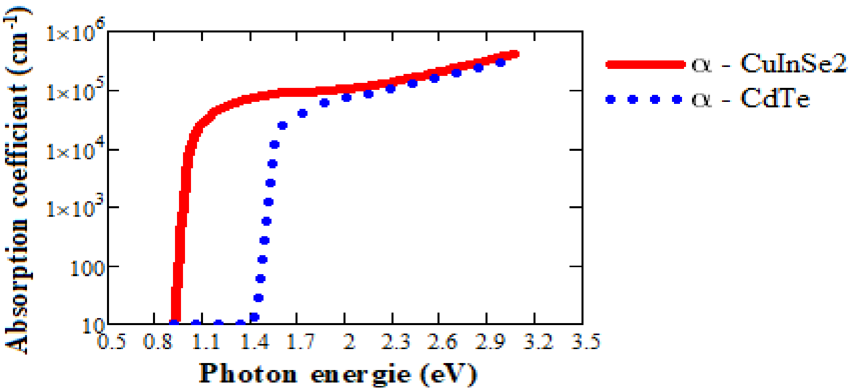

Figure 4: Evolution curve of the absorption coefficient as a function of energy

However, we note for some values of energy (1.04eV and 1.5eV) corresponding respectively to each material, an abrupt increase of the absorption coefficients up to a certain value (105 cm^{-1}) where an increase is observed. Indeed, these energy values correspond respectively to the gaps of these materials. For each material, we note an abrupt absorption.

Current-voltage characteristic of a solar cell

In this part, we apply the established results to plot the current-voltage characteristic noted J(V) (J is the photocurrent provided by the solar cell and V the voltage).

The figure 5 represents the evolution of the photocurrent density Jph and of the power of the solar cell P as a function of the voltage V for a homojunction deposited on the substrate in the presence of an additional electric field of the emitter.

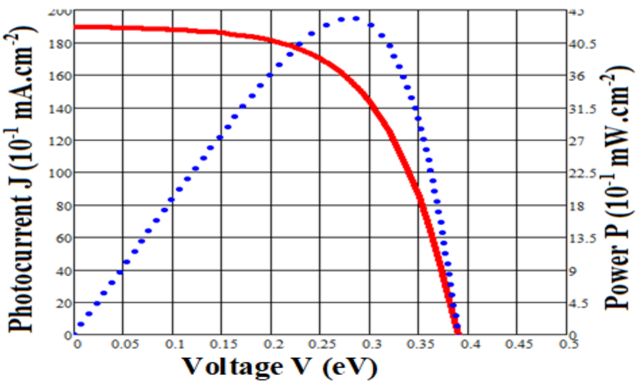

Figure 5: Jph(V) and P(V) characteristics of a photovoltaic cell

In Fig. 5, we note a maximum photocurrent density of approximately 27.5 mA.cm^{-2} at low values of the voltage (0V to 0.15V). It corresponds to the short-circuit photocurrent density. It decreases considerably until it vanishes for more elevated values of the voltage (0.25 to 0.5V). This is interpreted as a short-circuit where the maximum photocurrent is reaches and an open-circuit at the maximum voltage. For the curve of the power of the solar cell according to the voltage, the power of the solar cell varies linearly with the voltage up to the vicinity of the limit value which corresponds to the maximum power of the solar cell. When the voltage tends towards the value corresponding to the value of the open circuit, the power decreases until it cancels out.

The various electrical parameters characteristic of each model resulting from this study are summarized in Table 1.

Table 1: Values of the electrical parameters of the homojunction deposited on the substrate (CdTe) in the presence of an additional electric field in the emitter

Model	R_s ($\Omega.cm^2$)	R_{sh} ($\Omega.cm^2$)	J_{sc} ($mA.cm^{-2}$)	V_{oc} (V)	Jm ($mA.cm^{-2}$)	Vm (V)	Pm ($mW.cm^{-2}$)	FF	η_c (%)
Homojunction deposited substrate in the presence of an additional electric field	1	1000	30	0,42	24,43	0,30	7,329	0,582	7,87

Influence of series resistance Rs

In Figure 6, we have represented the evolution of the photocurrent density Jph in the case of the homojunction deposited on the substrate in the presence of an additional electric field in the emitter as a function of the voltage for different values of the series resistance Rs between 0 and 6 $\Omega.cm^2$. The shunt resistance Rsh is fixed at 1000$\Omega.cm^2$.

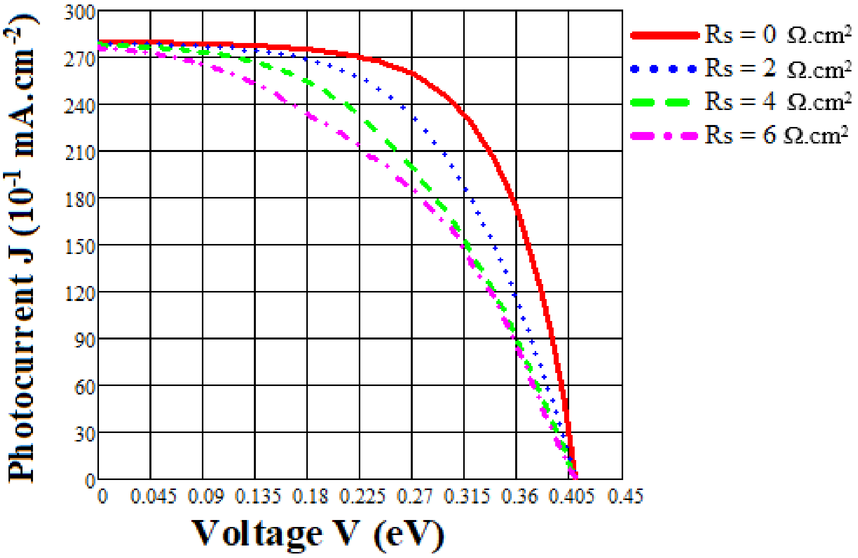

Figure 6: Influence of different values of series resistance on the J-V characteristic of an illuminated solar cell

In this figure 6, we note that the open circuit voltage (Voc) and the short circuit photocurrent (Jsc) are hardly modified. The characteristic deforms very quickly under the influence of Rs. This influence results in a decrease in the slope of the J-V characteristic in the area where the cell functions as a voltage source when Rs increases. The table 2 summarizes the electrical parameters of the cell by varying of the series resistance.

Table 2: Values of the electrical parameters for different values of the series resistance

Rs ($\Omega.cm^2$)	Rsh ($\Omega.cm^2$)	Jsc ($mA.cm^{-2}$)	η	Voc (V)	Jm ($mA.cm^{-2}$)	Vm (Ω)	Pm ($mW. cm^2$)	FF	η_c (%)
0	1000	30	2	0,41	26	0,306	7,968	0,632	8,56
2	1000	30	2	0,41	24,8	0,285	7,07	0,539	7,6
4	1000	30	2	0,41	26,8	0,245	6,569	0,464	7,05
6	1000	30	2	0,41	23	0,268	6,2	0,439	6,66

Influence of the shunt resistance Rsh

In Figure 7, we have represented the evolution of the photocurrent density Iph in the case of the homojunction deposited on the substrate in the presence of an additional electric field in the emitter as a function of the voltage for different values of the resistance Rsh shunt.

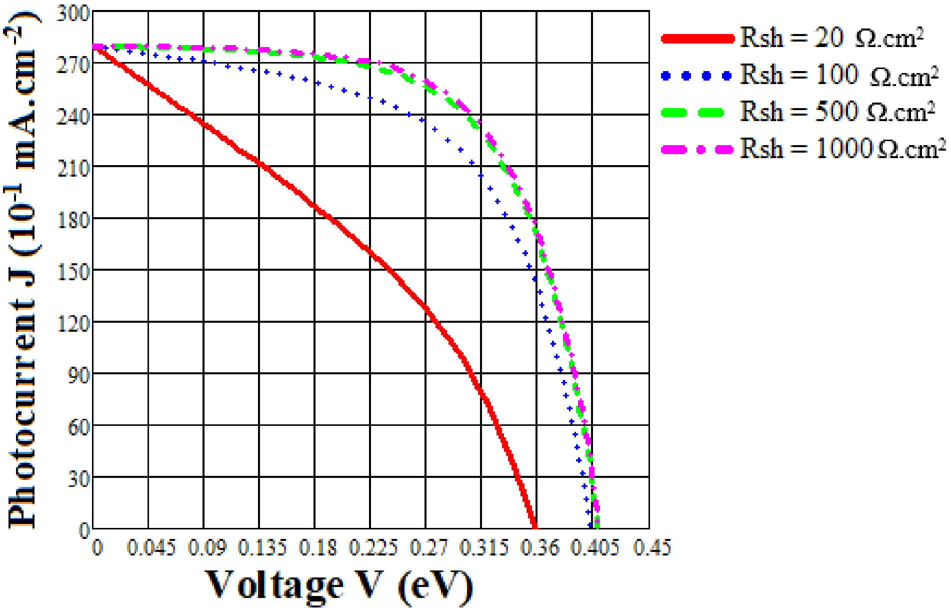

Figure 7: Influence of different values of shunt resistance on the J-V characteristic of an illuminated solar cell

In this figure 6, we notice that the short-circuit current is independent of the shunt resistance. While the open-circuit voltage depends on it. We also notice that for values of the shunt resistance greater than or equal to 100Ω.cm^2, the open-circuit voltage hardly varies. However, for values of the shunt resistance lower than 100Ω.cm^2, the influence of the shunt resistance is manifested by a reduction in the open-circuit voltage.

The results of the electrical parameters are mentioned in the following table 3 when increasing the shunt resistance.

Table 3: Values of the electrical parameters for different values of the shunt resistance

R_s (Ω.cm^2)	R_{sh} (Ω.cm^2)	J_{sc} (mA.cm^{-2})	η	V_{co} (V)	Jm (mA.cm^{-2})	Vm (Ω)	Pm (mW.cm^{-2})	FF	η_c (%)
1	20	30	2	0,357	17	0,225	4,074	0,36	4,37
1	100	30	2	0,402	21	0,31	7,115	0,579	7,64
1	500	30	2	0,409	23	0,315	7,872	0,633	8,45
1	1000	30	2	0,41	24	0,306	7,968	0,64	8,56

Effect of the ideality factor

In Figure 8, we have represented the evolution of the photocurrent density as a function of the voltage for different values of the ideality factor between [0.5;2] in the case of the homojunction deposited on the substrate in the presence of an additional electric field in the emitter.

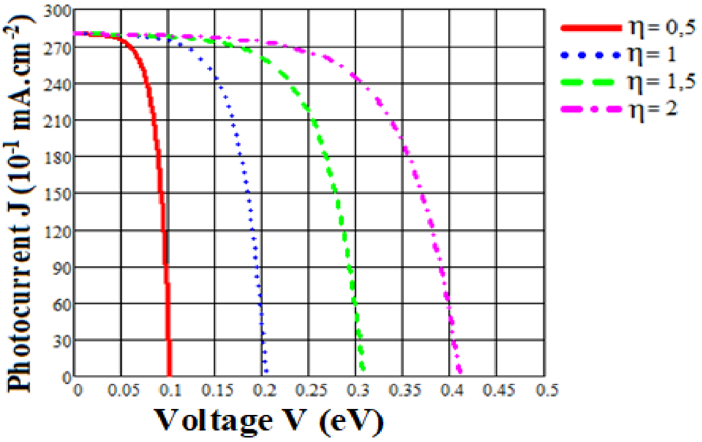

Figure 8: Influence of different values of the ideality factor on the J-V characteristic of an illuminated solar cell

We notice that the performance of the cell increases with the increase of the ideality factor. Indeed, this improvement is explained by the fact that the ideality factor reduces the diode current, which allows an increase in the open-circuit voltage.

Thus, the maximum power increases with the increase in the ideality factor.

The results of the electrical parameters are summarized in the following table 4 when increasing the ideality factor.

Table 4: Values of the electrical parameters for different values of the ideality factor

R_s (Ω.cm^2)	R_{sh} (Ω.cm^2)	J_{sc} (mA.cm^{-2})	η	V_{oc} (V)	Jm (mA.cm^{-2})	Vm (Ω)	Pm (mW.cm^{-2})	FF	η_c (%)
1	1000	28	0,5	0,102	18	0,077	1,42	0,65	1,5
1	1000	28	1	0,204	24	0,147	3,557	0,645	3,82
1	1000	28	1,5	0,308	24	0,23	5,501	0,641	5,91
1	1000	28	2	0,41	24	0,306	7,444	0,64	7,99

Conclusion

The study and optimization of the spectral responses of photovoltaic cells require knowledge of the geometric and electrical parameters of the structure studied. The photocurrent densities in each in the various regions of the cell were calculated, which allowed us to deduce the expressions of the J−V characteristics of the structure under consideration.

We have exposed the study of the influence of the J−V characteristics in order to optimize these parameters and consequently increase the conversion efficiency (≈ 8%) for a value of the ideality factor equal to 2.

This work aims to model and determine the spectral responses and the photovoltaic characteristics of the solar cell based on $CuInSe_2$, and also aims to enhance the performance of the cell by optimising the electrical and geometrical parameters

References

[1]. F. Therez, « Les Cellules Photovoltaïques au Silicium et à l’Arséniure de Galium : Modèles de Fonctionnement, Expérimentation et Application aux Générateurs sous Concentration », Thèse de Doctorat 3ème Cycle, LAAS, Toulouse 1984.

[2]. S. Madougou , F. Made, M.Boukary and G. Sissoko Recombination parameters Determination by Using Internal Quantum Effiency (IQE) Data on Bifacial Silicon Solar Cells ,Advanced Materials Research Vols. 18-19 pp. 314, (August 2007).

[3]. Zerbo, M. Zoungrana, A. D. Seré, F. Ouedraogo, R. Sam, B. Zouma, F. Zougmoré, « Influence d’une onde électromagnétique sur une photopile au silicium sous éclairement multispectral en régime statique », Revue des Energies Renouvelables Vol. 14 N°3 (2011), 517-532.

[4]. Zerbo, M. Zoungrana, A. D. Seré, F. Zougmoré, « Silicon solar cell under electromagnetic wave in steady state: effect of the telecommunication sources power of radiation, 2012 IOP Conf. Ser.: Mater. Sci. Eng. 29 012019.

[5]. B. MBOW, A. MEZERREG, N. REZZOUG and C. LLINARE, “Calculed and measure spectral response in near-infrarouge of III-V photo detectors based on Ga, In and Sb”. Physica Status Solidi (a) (1994) pp 513-514-515-523-524

[6]. E.M. Keita*, B. Mbow, M.L. Sow, C. Sow, M. Thiam, «Theoretical comparative study of internal quantum efficiency of thin films solar cells based on $CuInSe_2$: $P^+/P/N/N^+$, $P/N/N^+$, $P^+/P/N$ And P/N models» International Journal of Engineering science & Research Technology Vol. 5(9), 2016, pp 347-399.

[7]. C. Sow, B. Mbow, Y. Tabar, B. Ndiaye, M. Thiam, E.M. Keita ‘’ Theoretical study of internal quantum efficiency based on homojonction $CuInSe_2$ (n/p) with CdS window grown on CdTe substrate’’ International Journal of Engineering science & Research Technology Vol. 6(1), 2017, pp 140-153.

[8]. Laugier U.A. Roger, « Les photopiles solaires, technique et documentation », Ed 1981

[9]. Y. Tabar · M. L. Sow · E. M. Keita · A. A. Correa · B. Mbow, « Theoretical Study of Spectral Responses of Homojonctions Based on CuInSe2 Deposited on Substrate With or Without A Window Layer: Effect of An Electric Field », Journal of Materials Science & Surface Engineering, 6(4); 2018, pp 837-844

[10]. E. M. Keita, B. Mbow, M.S. Mane, M. L. Sow, C. Sow, C. Sene «Theoretical study of spectral responses of homojonctions based on CuInSe2» Journal of Materials Science & Surface Engineering Vol. 4(4), 2016, pp 392-399.

[11]. K. Boulahouata, « Modélisation d'une Cellule Solaire avec Etude Expérimentale », Mémoire de Fin d'Etudes (DES en Physique), Université de Tlemcen, 1998.

[12]. E. M. Keita, B. Mbow, C. Sene, '' Perovskites and other framework structure crystalline materials", chap No 22: Framework structure materials in photovoltaics based on perovskites 3D", OAJ Materials and Devices, vol 5 (2), (Coll. Acad. 2021), pp. 637-708.

[13]. Alain Ricaud, "Photopiles Solaires", de la physique de la conversion photovoltaique aux filieres, materiaux et procedes. 1997, 1e edition, Presses polytechniques et universitaires romandes, p. 40.

[14]. El Hadji Mamadou Keita*, Fallou Mbaye, Bachirou Ndiaye, Chamsdine Sow, Cheikh Sene, Babacar Mbow, "Optimizing Structures Based on Chalcopyrite Materials for Photovoltaic Applications", American Journal of Energy Engineering Vol.10 (3); 2022, pp. 53-67.

[15]. Mamadou Dia, Abdoul Aziz Correa, Chamsdine Sow, Elhadji Mamadou Keita, Babacar Mbow « Optimization of the Electrical Characteristics of the Photodiodes based on III-Sb Antimonide by a Ga1-yAly Sb Window layer Deposit at the Ga1-xInxSb Emitter Surface », American Journal of Engineering Research Vol. 10 (5), pp-378-384